

TURBULENT EXCHANGE OF MOMENTUM, MASS, AND HEAT BETWEEN FLUID STREAMS AND PIPE WALL

DARSHANLAL T. WASAN and CHARLES R. WILKE

Lawrence Radiation Laboratory and Department of Chemical Engineering,
University of California, Berkeley, California

(Received 28 May 1963)

Abstract—A new correlation is presented to describe mass and heat transfer to a fluid in a fully developed turbulent flow in a pipe. The correlation differs from earlier empirical relations in that it is based on a theoretical continuous eddy-viscosity distribution from the wall to the center of the pipe. Transfer rates calculated from the new correlation are in excellent agreement with experimental data on mass and heat transfer to fluid streams.

NOMENCLATURE

C ,	concentration of diffusing species;
C_w ,	concentration at the wall;
C_{avg} ,	time-average concentration;
C_p ,	heat capacity;
D ,	molecular diffusivity;
F ,	functional notation;
g_c ,	conversion constant;
k_c ,	mass-transfer coefficient;
Nu ,	Nusselt number;
Pr ,	Prandtl number;
Sc ,	Schmidt number;
St ,	Stanton number;
T_w ,	temperature at the wall;
T ,	temperature;
T_{avg} ,	average temperature;
U^+ ,	dimensionless velocity;
y ,	distance from the wall;
y^+ ,	yU_τ/ν ;
μ ,	molecular viscosity;
ν ,	kinematic viscosity;
ρ ,	density of fluid;
ϵ_v ,	eddy viscosity;
ϵ_d ,	eddy diffusivity for mass;
ϵ_c ,	eddy conductivity;
τ_w ,	shear stress at the wall;
St_m ,	Stanton number for mass;
St_h ,	Stanton number for heat;
u ,	fluctuating velocity in the axial direction;
v ,	fluctuating velocity in the radial direction;

\overline{uv} , Reynolds stress.

INTRODUCTION

THE turbulent exchange of momentum, mass, and heat in the vicinity of a boundary is encountered in many engineering processes. It is well established [1, 2, 3] that in the vicinity of a boundary the turbulent exchange of momentum, mass, and heat is governed not only by molecular motion but also by an eddy motion. To predict rates of mass and heat transfer between a moving fluid and a wall it is therefore essential to understand the mechanism of eddy motion in the vicinity of a wall. Unfortunately very little is known about the distribution of eddies very close to the wall. In the past, due to the absence of both theoretical analyses and experimental data for the region close to the wall, a number of empirical expressions have been proposed for eddy-viscosity distributions near a wall. An excellent review of several such existing correlations for fully developed turbulent flow in a pipe with constant fluid properties has been presented by Sherwood [3].

Recently Wasan, Tien, and Wilke [4] pointed out that most of the proposed eddy-viscosity distributions do not satisfy the theoretical criterion which states that the turbulent contribution to Reynolds stress \overline{uv} near the wall is proportional to y^n where n is not less than three. This criterion was first derived by Townsend [5]. Also, all the previous analyses are based on the

concept of three sharply defined fluid layers, namely laminar sublayer, buffer, and turbulent layers. However, according to these authors [4], and also Gowariker [6], this concept of three different fluid layers leads to an unrealistic discontinuity in the value of the eddy-viscosity function with respect to that obtained from logarithmic distribution in the turbulent core. Rannie [7] and Sleicher [8] in their analyses avoided this point of discontinuity, but the eddy-viscosity functions of both of these authors do not give satisfactory relationships for analogy expressions for heat- and mass-transfer rates for systems with high Schmidt or Prandtl numbers. From velocity-variation data and from turbulent shear-stress data of Laufer [9] it is evident that the degree of turbulence in the moving fluid varies continuously from the wall to the axis of a pipe. Hence, the concept of three distinct fluid layers would appear to be incorrect.

By using the equations of mean motion and the well established empirical logarithmic velocity distribution in the turbulent core, Wasan, Tien, and Wilke [4] have derived theoretical expressions for the continuous variation of velocity and eddy viscosity for the wall region of pipe flow. The distributions of these authors fit the experimental data on velocity and turbulent shear stress over the wall region. Their velocity and eddy-viscosity distributions for the wall region ($0 \leq y^+ \leq 20$) are presented in equations (1) and (2) as follows:

$$U^+ = y^+ - 1.04 \times 10^{-4} y^{+4} + 3.03 \times 10^{-6} y^{+5}, \quad (1)$$

and

$$\frac{\epsilon_v}{\nu} = \frac{4.16 \times 10^{-4} y^{+3} - 15.15 \times 10^{-6} y^{+4}}{1 - 4.16 \times 10^{-4} y^{+3} + 15.15 \times 10^{-6} y^{+4}} \quad (2)$$

We present correlations relating the fluid friction and turbulent-exchange rates of mass and heat over a wide range of Schmidt and Prandtl numbers based on these distributions. The corresponding concentration and temperature distributions for the wall region of pipe flow are also presented.

ANALYSIS

Consider a fully developed turbulent flow of fluid with constant properties in a pipe having

walls kept at a constant concentration C_W or at a constant temperature T_W . Mass or heat is transferred to the fluid stream both by molecular and by eddy motions. As is customary, the shear-stress, mass-transfer, and heat-transfer fluxes can be written as the sum of molecular and turbulent fluxes as follows:

$$\tau g_c = (\mu + \rho \epsilon_v) \frac{dU}{dy}, \quad (3)$$

$$N_A = (D + \epsilon_d) \frac{dC}{dy}, \quad (4)$$

and

$$q = \rho c p (k + \epsilon_c) \frac{dT}{dy}, \quad (5)$$

where τ is the shear stress at a plane parallel to the wall, N_A is the mass flux, and q is the heat flux across a plane parallel to the wall.

To solve (3), (4) and (5), several assumptions are usually made [3]. First, in the wall region the shear stress τ , mass-transfer flux N_A , and heat-transfer flux q are assumed to be constant and equal to the value at the wall. Second, in the fully turbulent region the variation of shear stress, mass transfer, and heat transfer is such that τ/N_A and τ/q are constant, and molecular viscosity μ , molecular diffusivity D and thermal conductivity k can be neglected. Third, in the case of mass transfer the interfacial velocity is assumed to be negligible. The last important assumption is that eddy diffusivities of momentum ϵ_v , mass ϵ_d and heat ϵ_c are equal.

Now, by combinations of (3) and (4) and after integration, for the turbulent region one obtains

$$\frac{C_{avg} - C_1}{U_{avg} - U_1} = \frac{\rho N_{AW}}{\tau w g_c}, \quad (6)$$

where C_{avg} and U_{avg} refer to the average concentration and velocity respectively, and C_1 and U_1 refer to concentration and velocity each corresponding to $y^+ = 20$. After combining (1) and (6) one gets

$$C_{avg} - C_1 = \frac{\rho}{\tau w g_c} N_{AW} U_{avg} [1 - 13.0 \sqrt{(f/2)}], \quad (7)$$

where the concentration C_1 corresponding to $y^+ = 20$ is determined as follows:

In the wall region equation (4) can be re-written as

$$N_{AW} = \sqrt{\left(\frac{\tau_w g_c}{\rho}\right)} \left(\frac{1}{Sc} + \frac{\epsilon_v}{\nu}\right) \frac{dC}{dy^+}. \quad (8)$$

Integration of (8) gives

$$C_1 - C_W = \frac{N_{AW}}{\sqrt{(\tau_w g_c/\rho)}} \int_0^{20} \frac{dy^+}{(1/Sc + \epsilon/\nu)}. \quad (9)$$

Therefore, from (7) and (9) there results

$$C_{avg} - C_W = \frac{\rho N_{AW}}{\tau_w g_c} U_{avg} [1 - 13.0 \sqrt{(f/2)}] + \frac{N_{AW}}{\sqrt{(\tau_w g_c/\rho)}} \int_0^{20} \frac{dy^+}{(1/Sc + \epsilon/\nu)}. \quad (10)$$

But the mass flux N_{AW} at the wall can be given by the expression

$$N_{AW} = k_c (C_{avg} - C_W). \quad (11)$$

Hence, from (10) and (11) the expression for mass-transfer Stanton number in terms of Schmidt number and friction factor becomes

$$St_m = \frac{k_c}{U_{avg}} = \frac{f/2}{1 + \sqrt{(f/2)} \left[\int_0^{20} \frac{dy^+}{(1/Sc + \epsilon/\nu)} - 13.0 \right]}, \quad (12)$$

where ϵ/ν is given by equation (2).

Similarly from (3) and (5) the expression for heat-transfer Stanton number in terms of Prandtl number and friction factor can be obtained as

$$St_h = \frac{f/2}{1 + \sqrt{(f/2)} [F(Pr, 20) - 13.0]} \quad (13)$$

CONCENTRATION AND TEMPERATURE DISTRIBUTIONS

When (8) and (10) are combined, the expression for the concentration distribution becomes

$$\frac{C - C_W}{C_{avg} - C_W} = \frac{F(Sc, y^+)}{F(Sc, 20) + \sqrt{(2/f)} - 13.0} \quad (14)$$

Similarly the temperature distribution is obtained as

$$\frac{T - T_W}{T_{avg} - T_W} = \frac{F(Pr, y^+)}{F(Pr, 20) + \sqrt{(2/f)} - 13.0}, \quad (15)$$

where

$$F(Pr, y^+) = \int_0^{y^+} \frac{dy^+}{[1/Pr + \epsilon/\nu(y^+)]}. \quad (16)$$

Equations (14), (15) and (16) give the concentration and temperature distributions in the wall region of a pipe flow.

The functions $F(Sc$ or $Pr, y^+)$ and $F(Sc$ or $Pr, 20)$ appearing in (13) and (15) involve the integrals which cannot be solved in closed forms. These were obtained by numerical integration using Simpson's one-third rule with a digital computer. These functions are shown in Table 1 for Sc or Pr numbers over a range of 0.1 to 10 000.

DISCUSSION

In Fig. 1 the function $F(Sc, y^+)$ or $F(Pr, y^+)$ is shown for the range of Schmidt and Prandtl

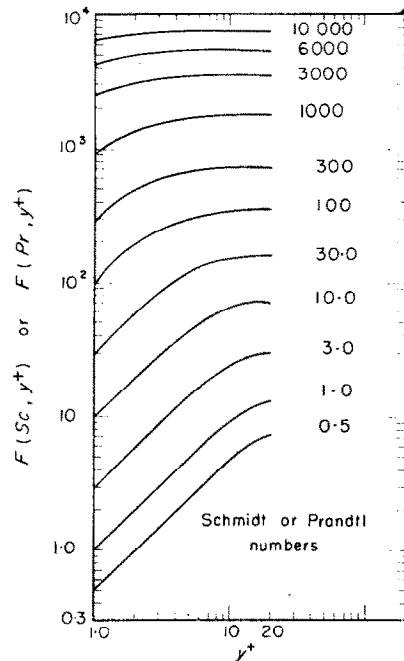


FIG. 1. Plot of $F(Sc, y^+)$ or $F(Pr, y^+)$ vs. y^+ .

Table 1. Tabulation of functions $F(Sc, y^+)$ or $F(Pr, y^+)$ = $\int_0^{y^+} \frac{dy^+}{Sc} + \frac{\epsilon(y^+)}{y}$

Sc or Pr	1	2	3	4	5	6	7	8	9	10	11	12	13	14	15	16	17	18	19	20	
0.1	0.1	0.2	0.3	0.4	0.5	0.6	0.7	0.8	0.9	1.0	1.1	1.2	1.3	1.4	1.5	1.6	1.7	1.8	1.9	2.0	
0.2	0.2	0.4	0.6	0.8	1.0	1.2	1.4	1.6	1.8	2.0	2.1	2.3	2.5	2.7	2.8	3.0	3.1	3.2	3.3	3.4	3.5
0.3	0.3	0.6	1.0	1.5	2.0	2.4	2.8	3.1	3.5	3.9	4.2	4.5	4.8	5.1	5.4	5.6	5.8	5.9	6.0	6.1	6.4
0.4	0.4	0.8	1.2	2.0	3.0	3.6	4.1	4.7	5.2	5.7	6.2	6.6	7.0	7.4	7.7	8.0	8.2	8.4	8.5	8.6	9.1
0.5	0.5	1.0	1.8	3.0	4.5	5.2	6.1	7.1	8.1	9.1	10.1	11.0	11.9	12.8	13.5	14.1	14.5	14.8	14.9	15.0	16.0
0.6	0.6	1.4	2.4	4.5	7.5	9.0	11.0	13.4	16.0	18.6	21.3	24.1	26.8	29.4	31.8	33.8	35.2	36.2	36.9	37.8	42.0
0.7	0.7	1.6	2.7	5.2	8.9	11.3	14.2	17.7	21.6	25.5	29.4	33.3	37.0	40.5	43.7	46.6	49.2	51.6	53.8	56.6	64.0
0.8	0.8	1.8	2.9	5.7	9.9	12.8	16.1	19.8	24.1	28.4	32.7	36.9	40.9	44.5	47.7	50.6	53.2	55.7	58.1	60.5	71.0
0.9	0.9	2.0	3.0	6.4	11.1	14.4	18.2	22.4	27.0	31.7	36.4	41.0	45.5	49.0	51.7	54.4	56.9	59.4	61.8	64.2	77.0
1.0	1.0	2.2	3.2	6.9	12.3	16.0	20.1	24.6	29.4	34.1	38.8	43.4	47.9	51.4	54.0	56.6	59.1	61.6	64.0	66.4	80.0
1.1	1.1	2.4	3.4	7.4	13.0	17.0	21.4	26.0	30.8	35.5	40.1	44.7	49.2	52.7	55.3	57.9	60.4	62.9	65.3	67.7	82.0
1.2	1.2	2.6	3.6	8.0	13.8	18.0	22.6	27.4	32.2	36.9	41.5	46.1	50.6	54.1	56.7	59.3	61.8	64.3	66.7	69.1	84.0
1.3	1.3	2.8	3.8	8.6	14.6	19.0	23.6	28.6	33.4	38.1	42.7	47.3	51.8	55.3	57.9	60.5	63.0	65.5	67.9	70.3	86.0
1.4	1.4	3.0	4.0	9.2	15.4	20.0	24.7	29.6	34.3	38.9	43.5	48.1	52.6	56.1	58.7	61.3	63.9	66.4	68.9	71.3	88.0
1.5	1.5	3.2	4.2	9.8	16.2	21.0	25.8	30.8	35.5	40.1	44.7	49.2	53.7	57.2	59.8	62.4	65.0	67.6	70.1	72.7	90.0
1.6	1.6	3.4	4.4	10.4	17.0	22.0	26.9	31.9	36.5	41.1	45.7	50.2	54.7	58.2	60.8	63.4	66.0	68.6	71.1	73.7	92.0
1.7	1.7	3.6	4.6	11.0	17.8	23.0	28.0	33.1	37.6	42.2	46.8	51.3	55.8	59.3	61.9	64.5	67.1	69.7	72.3	74.9	94.0
1.8	1.8	3.8	4.8	11.6	18.6	24.0	29.1	34.3	38.7	43.3	47.9	52.4	56.9	60.4	63.0	65.6	68.2	70.8	73.4	76.0	96.0
1.9	1.9	4.0	5.0	12.2	19.4	25.0	30.2	35.5	39.8	44.3	48.9	53.4	57.9	61.4	64.0	66.6	69.2	71.8	74.4	77.0	98.0
2.0	2.0	4.2	5.2	12.8	20.2	26.0	31.3	36.6	40.9	45.9	50.5	55.0	59.5	63.0	65.6	68.2	70.8	73.4	76.0	78.6	100.0
2.1	2.1	4.4	5.4	13.4	21.0	27.0	32.4	37.7	41.9	46.9	51.5	56.0	60.5	64.0	66.6	69.2	71.8	74.4	77.0	79.6	102.0
2.2	2.2	4.6	5.6	14.0	21.8	28.0	33.4	38.8	42.9	47.9	52.5	57.0	61.5	65.0	67.6	70.2	72.8	75.4	78.0	80.6	104.0
2.3	2.3	4.8	5.8	14.6	22.6	29.0	34.4	39.9	43.9	48.9	53.5	58.0	62.5	66.0	68.6	71.2	73.8	76.4	79.0	81.6	106.0
2.4	2.4	5.0	6.0	15.2	23.4	30.0	35.4	41.0	44.9	49.9	54.5	59.0	63.5	67.0	69.6	72.2	74.8	77.4	80.0	82.6	108.0
2.5	2.5	5.2	6.2	15.8	24.2	31.0	36.4	42.1	46.0	51.0	55.5	60.0	64.5	68.0	70.6	73.2	75.8	78.4	81.0	83.6	110.0
2.6	2.6	5.4	6.4	16.4	25.0	32.0	37.4	43.2	47.1	52.1	56.5	61.0	65.5	69.0	71.6	74.2	76.8	79.4	82.0	84.6	112.0
2.7	2.7	5.6	6.6	17.0	25.8	33.0	38.4	44.3	48.2	53.2	57.5	62.0	66.5	70.0	72.6	75.2	77.8	80.4	83.0	85.6	114.0
2.8	2.8	5.8	6.8	17.6	26.6	34.0	39.4	45.4	49.3	54.3	58.5	63.0	67.5	71.0	73.6	76.2	78.8	81.4	84.0	86.6	116.0
2.9	2.9	6.0	7.0	18.2	27.4	35.0	40.4	46.5	50.4	55.4	59.5	64.0	68.5	72.0	74.6	77.2	79.8	82.4	85.0	87.6	118.0
3.0	3.0	6.2	7.2	18.8	28.2	36.0	41.4	47.6	51.4	56.4	60.5	65.0	69.5	73.0	75.6	78.2	80.8	83.4	86.0	88.6	120.0
3.1	3.1	6.4	7.4	19.4	29.0	37.0	42.4	48.7	52.4	57.4	61.5	66.0	70.5	74.0	76.6	79.2	81.8	84.4	87.0	89.6	122.0
3.2	3.2	6.6	7.6	20.0	29.8	38.0	43.4	49.8	53.4	58.4	62.5	67.0	71.5	75.0	77.6	80.2	82.8	85.4	88.0	90.6	124.0
3.3	3.3	6.8	7.8	20.6	30.6	39.0	44.4	50.9	54.4	59.4	63.5	68.0	72.5	76.0	78.6	81.2	83.8	86.4	89.0	91.6	126.0
3.4	3.4	7.0	8.0	21.2	31.4	40.0	45.4	52.0	55.4	60.4	64.5	69.0	73.5	77.0	79.6	82.2	84.8	87.4	90.0	92.6	128.0
3.5	3.5	7.2	8.2	21.8	32.2	41.0	46.4	53.1	56.4	61.4	65.5	70.0	74.5	78.0	80.6	83.2	85.8	88.4	91.0	93.6	130.0
3.6	3.6	7.4	8.4	22.4	33.0	42.0	47.4	54.2	57.4	62.4	66.5	71.0	75.5	79.0	81.6	84.2	86.8	89.4	92.0	94.6	132.0
3.7	3.7	7.6	8.6	23.0	33.8	43.0	48.4	55.3	58.4	63.4	67.5	72.0	76.5	80.0	82.6	85.2	87.8	90.4	93.0	95.6	134.0
3.8	3.8	7.8	8.8	23.6	34.6	44.0	49.4	56.4	59.4	64.4	68.5	73.0	77.5	81.0	83.6	86.2	88.8	91.4	94.0	96.6	136.0
3.9	3.9	8.0	9.0	24.2	35.4	45.0	50.4	57.5	60.4	65.4	69.5	74.0	78.5	82.0	84.6	87.2	89.8	92.4	95.0	97.6	138.0
4.0	4.0	8.2	9.2	24.8	36.2	46.0	51.4	58.6	61.4	66.4	70.5	75.0	79.5	83.0	85.6	88.2	90.8	93.4	96.0	98.6	140.0
4.1	4.1	8.4	9.4	25.4	37.0	47.0	52.4	59.7	62.4	67.4	71.5	76.0	80.5	84.0	86.6	89.2	91.8	94.4	97.0	99.6	142.0
4.2	4.2	8.6	9.6	26.0	37.8	48.0	53.4	60.8	63.4	68.4	72.5	77.0	81.5	85.0	87.6	90.2	92.8	95.4	98.0	100.6	144.0
4.3	4.3	8.8	9.8	26.6	38.6	49.0	54.4	61.9	64.4	69.4	73.5	78.0	82.5	86.0	88.6	91.2	93.8	96.4	99.0	101.6	146.0
4.4	4.4	9.0	10.0	27.2	39.4	50.0	55.4	63.0	65.4	70.4	74.5	79.0	83.5	87.0	89.6	92.2	94.8	97.4	100.0	102.6	148.0
4.5	4.5	9.2	10.2	27.8	40.2	51.0	56.4	64.1	66.4	71.4	75.5	80.0	84.5	88.0	90.6	93.2	95.8	98.4	101.0	103.6	150.0
4.6	4.6	9.4	10.4	28.4	41.0	52.0	57.4	65.2	67.4	72.4	76.5	81.0	85.5	89.0	91.6	94.2	96.8	99.4	102.0	104.6	152.0
4.7	4.7	9.6	10.6	29.0	41.8	53.0	58.4	66.3	68.4	73.4	77.5	82.0	86.5	90.0	92.6	95.2	97.8	100.4	103.0	105.6	154.0
4.8	4.8	9.8	10.8	29.6	42.6	54.0	59.4	67.4	69.4	74.4	78.5	83.0	87.5	91.0	93.6	96.2	98.8	101.4	104.0	106.6	156.0
4.9	4.9	10.0	11.0	30.2	43.4	55.0	60.4	68.4	70.4	75.4	79.5	84.0	88.5	92.0	94.6	97.2	99.8	102.4	105.0	107.6	158.0
5.0	5.0	10.2	11.2	30.8	44.2	56.0	61.4	69.4	71.4	76.4	80.5	85.0	89.5	93.0	95.6	98.2	100.8	103.4	106.0	109.0	160.0
5.1	5.1	10.4	11.4	31.4	45.0	57.0	62.4	70.4	72.4	77.4	81.5	86.0	90.5	94.0	96.6	99.2	101.8	104.4	107.0	110.6	162.0
5.2	5.2	10.6	11.6	32.0	45.8	58.0	63.4	71.4	73.4	78.4	82.5	87.0	91.5	95.0	97.6	100.2	102.8	105.4	108.0	111.6	164.0
5.3	5.3	10.8	11.8	32.6	46.6	59.0	64.4	72.4	74.4	79.4	83.5	88.0	92.5	96.0	98.6	101.2	103.8	106.4	109.0	112.6	166.0
5.4	5.4	11.0	12.0	33.2	47.4	60.0	65.4	73.4	75.4	80.4	84.5	89.0	93.5	97.0	99.6	102.2	104.8	107.4	110.0	113.6	168.0
5.5	5.5	11.2	12.2	33.8	48.2	61.0	66.4	74.4	76.4	81.4	85.5	90.0	94.5	98.0	100.6	103.2	105.8	108.4	111.0	114.6	170.0
5.6	5.6	11.4	12.4	34.4	49.0	62.0	67.4	75.4	77.4	82.4	86.5	91.0	95.5	99.0	101.6	104.2	106.8	109.4	112.0	115.6	172.0
5.7	5.7	11.6	12.6	35.0	49.8	63.0	68.4	76.4	78.4	83.4	87.5	92.0	96.5	100.0	102.6	105.2	107.8	110.4	113.0	116.6	174.0
5.8	5.8	11.8	12.8	35.6	50.6	64.0	69.4	77.4	79.4	84.4	88.5	93.0	97.5	101.0	103.6	106.2	108.8	111.4	114.0	117.6	176.0
5.9	5.9	12.0	13.0	36.2	51.4	65.0	70.4	78.4	80.4	85.4	89.5	94.0	98.5	102.0	104.6	107.2	109.8	112.4	115.0	118.6	178.0
6.0	6.0	12.2	13.2	36.8	52.2	66.0	71.4	79.4	81.4	86.4	90.5	95.0	99.5	103.0	105.6	108.2	110.8	113.4	116.0	119.6	180.0

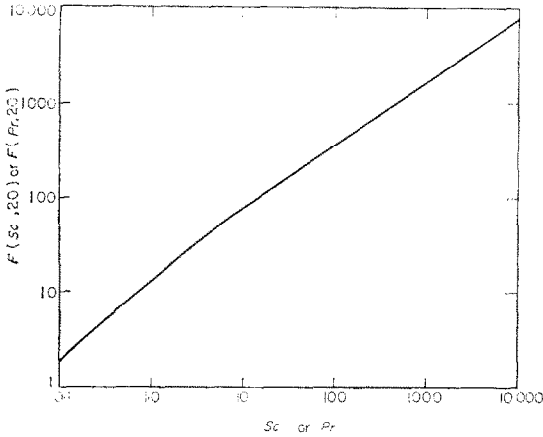


FIG. 2. Plot of $F(Sc)$ vs. Sc or $F(Pr)$ vs. Pr .

numbers from 0.5 to 10 000. Fig. 2 shows the calculated values of the function $F(Sc, 20)$ or $F(Pr, 20)$. For rapid calculation purposes the function shown on Fig. 2 can be approximated with a maximum error of ± 2 per cent as follows:

For turbulent diffusion in gases the function $F(Sc, 20)$ can be represented by the equation

$$F(Sc, 20) = 13.0 (Sc)^{0.80}, \text{ where } 0.2 \leq Sc \leq 2. \tag{17}$$

For diffusion in liquid streams the following equation is proposed:

$$F(Sc, 20) = 17.25 (Sc)^{0.66}, \text{ where } 100 \leq Sc \leq 10\,000. \tag{18}$$

For the intermediate range of Schmidt and Prandtl numbers the function F can be given by the equation

$$F(Sc, 20) = 13.8 (Sc)^{0.71}, \text{ where } 2 \leq Sc \leq 100. \tag{19}$$

In Figs. 3 and 4 the proposed mass- and heat-transfer Stanton-number relationship is compared with heat- and mass-transfer data of many workers at Reynolds numbers of 10 000 and 25 000. The experimental points representing a mean through the data are the ones chosen by Deissler except for the datum point of Meyerink and Friedlander [11] which was taken from their mean curve through the data. The proposed expression agrees very well with the data over a wide range of Schmidt and Prandtl numbers.

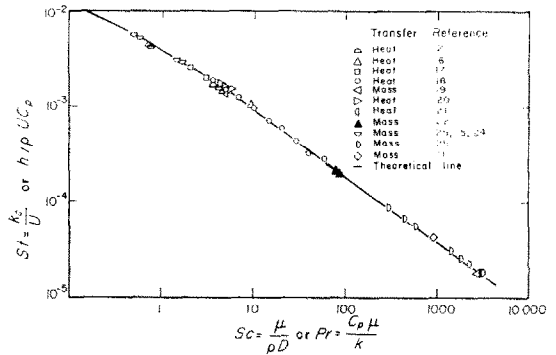


FIG. 3. Comparison of present theory with experimental data at a Reynolds number of 10 000.

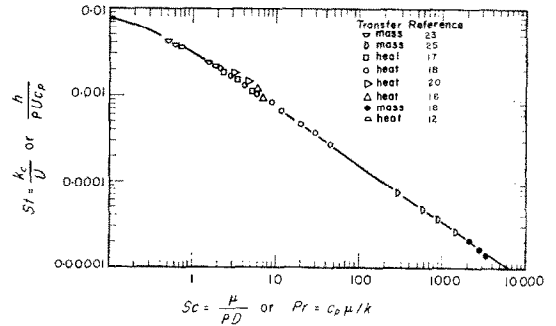


FIG. 4. Comparison of present theory with experimental data at a Reynolds number of 25 000.

Fig. 5 shows a comparison of the values calculated from the proposed Stanton number relationship at a Reynolds number of 50 000 with those calculated from the expressions of Deissler [10], Gowariker [6], Lin, Moulton and Putnam [13], Rannie [7], and von Kármán [14]. It is noted that von Kármán's relationship

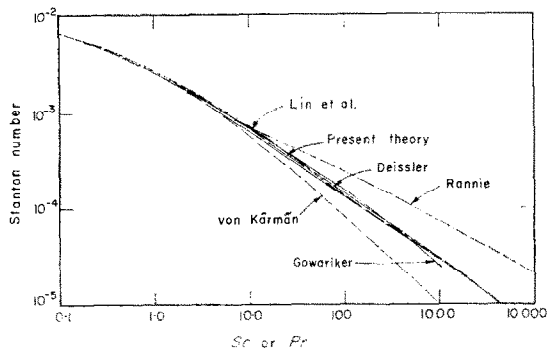


FIG. 5. Comparison of several analogies at a Reynolds number of 50 000.

gives too low results and Rannie's expression gives too high results at large Schmidt and Prandtl numbers. However, our correlation agrees very well with those of Lin, Moulton and Putnam, and Deissler.

By combinations of (12) and (18), we express Stanton number in terms of Schmidt number and friction factor for large values of Schmidt number by

$$St_m = 0.058 \sqrt{(f/2)} (Sc)^{-0.66} \quad (20)$$

It is of interest that the exponent on the Schmidt number as given by (20) is in agreement with the Chilton and Colburn analogy [15].

The curves for heat and mass transfer expressed in the form of Nusselt numbers are shown in Fig. 6. The Nusselt number for mass transfer (i.e. the Sherwood number) can be correlated by the following expressions:

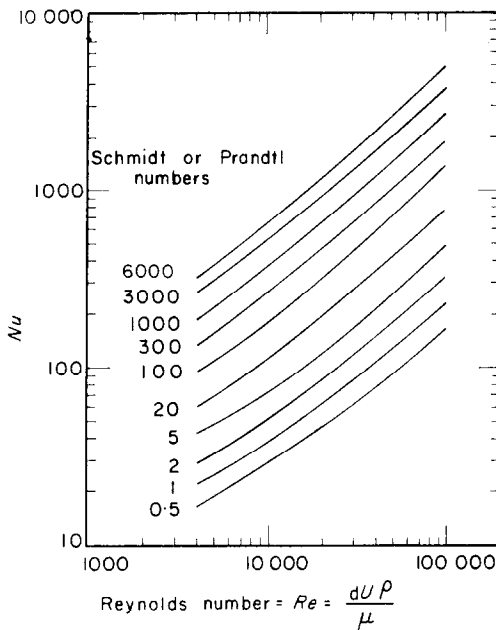


FIG. 6. Nusselt number vs. Reynolds number at various Schmidt or Prandtl numbers.

$$Nu = \frac{(f/2) (Re) (Sc)}{1 + \sqrt{(f/2)} [13.0(Sc)^{0.80} - 13.0]} \quad \text{for } 0.2 \leq Sc \leq 2, \quad (21)$$

$$Nu = \frac{(f/2) (Re) (Sc)}{1 + \sqrt{(f/2)} [13.8(Sc)^{0.71} - 13.0]} \quad \text{for } 2 \leq Sc \leq 100, \quad (22)$$

$$\text{and } Nu = (0.058) \sqrt{(f/2)} (Re) (Sc)^{0.34} \quad \text{for } 100 \leq Sc \leq 10\,000. \quad (23)$$

Heat transfer Nusselt numbers can be obtained by replacing Schmidt numbers by Prandtl numbers in the above expressions. These expressions for Nusselt numbers are based on the difference between wall and average concentration or temperature.

CONCLUSIONS

We show that agreement between predicted values and experimental data of mass- and heat-transfer rates supports the use of the proposed eddy-viscosity distribution function. Our predicted transfer rates agree very well with those calculated from Lin, Moulton and Putnam relationships, which are in excellent agreement with experimental data. Our proposed eddy-viscosity expression is useful because it applies to the whole wall region of pipe flow and is developed on a sound theoretical basis. It would also appear that the previous concept of sharply defined fluid layers is not necessary.

To calculate mass- and heat-transfer rates, simplified equations in the form of equations (17), (18) and (19) can be used to predict the complicated functions $F(Sc)$ and $F(Pr)$. Also, simplified equations in the form of equations (21), (22) and (23) are proposed to predict heat- and mass-transfer Nusselt-number relationships.

REFERENCES

1. A. FAGE and H. C. TOWNEND, *Proc. Roy. Soc. London* **135**, 656 (1932).
2. T. J. HANRATTY, *A.I.Ch.E. J.* **2**, 359 (1956).
3. T. K. SHERWOOD, *Chem. Engng. Progr. Symposium Series*, **55**, 71 (1959).
4. D. T. WASAN, C. L. TIEN and C. R. WILKE, *A.I.Ch.E.J.* **9**, 567 (1963).
5. A. A. TOWNSEND, *The Structure of Turbulent Shear Flow*. Cambridge University Press (1956).
6. V. R. GOWARIKER, U.K. Atom. Energy Comm. AERE 1055 (1962).
7. W. D. RANNIE, *J. Aero. Sci.* **23**, 485 (1956).
8. C. A. SLEICHER, *Trans. ASME* **80**, 693 (1958).
9. J. LAUFER, Natl. Advisory Comm. Aeron. Tech. Report 1174 (1954).
10. R. G. DEISSLER, Natl. Advisory Comm. Aeron. Tech. Report 1210 (1955).
11. E. S. C. MEYERINK and S. K. FRIEDLANDER, National Science Foundation Report Grant No. G5079 (May 1960).

12. R. G. DEISSLER and C. S. EIAN, Natl. Advisory Comm. Aeron. TN 2629 (1952).
13. C. S. LIN, R. W. MOULTON and G. L. PUTNAM, *Industr. Engng. Chem.* **45**, 636 (1953).
14. T. VON KÁRMÁN, *Trans. ASME* **61**, 705 (1939).
15. T. H. CHILTON and A. P. COLBURN, *Industr. Engng. Chem.* **26**, 1183 (1934).
16. A. E. EAGLE and R. M. FERGUSON, *Proc. Roy. Soc. London* **127**, 540 (1930).
17. F. KREITH and M. SUMMERFIELD, *Trans. ASME* **72**, 869 (1950).
18. E. BERNARDO and S. EIAN, Natl. Advisory Comm. Aeron. WRE 136 (1945).
19. W. H. LINTON and T. K. SHERWOOD, *Chem. Engng. Progr.* **46**, 258 (1950).
20. M. D. GRELE and L. GREDEON, Natl. Advisory Comm. Aeron. RM E 53Lo9 (1953).
21. H. W. HOFFMAN, Oakridge Natl. Laboratory Report 1370, Contract No. W-7405-eng-26 (1952).
22. C. F. BONILLA, NYO-3086, U.S. Atom. Energy Comm. AEC Contract No. AT 30-1-1100 (1951).
23. W. I. BARNET and K. A. KOBE, *Industr. Engng. Chem.* **33**, 436 (1941).
24. M. L. JACKSON and N. H. CEOGLSKE, *Industr. Engng. Chem.* **42**, 1188 (1950).
25. C. S. LIN, E. B. DENTON, H. S. GASKIL and G. L. PUTNAM, *Industr. Engng. Comm.* **43**, 2136 (1951).
26. S. J. KAUFMAN and F. D. SELY, Natl. Advisory Comm. Aeron. RME 50G 31 (1950).

Résumé—Les auteurs présentent une nouvelle expression du transport de chaleur et de masse pour un fluide en écoulement pleinement turbulent dans une conduite. Cette expression diffère des relations empiriques précédentes en ce qu'elle est établie à partir d'une distribution de viscosité turbulente continue de la paroi vers le centre de la conduite. Les coefficients de transport calculés à partir de la nouvelle corrélation sont en excellent accord avec les données expérimentales de transport de chaleur et de masse dans les écoulements fluides.

Zusammenfassung—Zum Beschreiben des Stoff- und Wärmeüberganges an ein Fluid in voll entwickelter turbulenter Rohrströmung wird eine neue Beziehung angegeben. Von älteren empirischen Beziehungen unterscheidet sie sich dadurch, dass sie auf einer theoretischen kontinuierlichen Verteilung der Wirbelviskosität von der Rohrwand bis zur Achse beruht. Mittels dieser neuen Beziehung berechnete Übergangswerte stimmen mit Versuchsergebnissen ausgezeichnet überein.

Аннотация—Дается новое соотношение для описания процесса переноса тепла и вещества к жидкости при полностью развитом турбулентном течении в трубе. Это соотношение отличается от предыдущих эмпирических соотношений тем, что оно основано на теоретическом распределении турбулентной вязкости от стенки к центру трубы. Скорости переноса, вычисленные с помощью новой корреляции, хорошо согласуются с экспериментальными данными по переносу тепла и массы к потокам жидкости.